

RESEARCH ARTICLE

A Crowdsourcing Approach to Developing and Assessing Prediction Algorithms for AML Prognosis

David P. Noren¹, Byron L. Long¹, Raquel Norel², Kahn Rrhissorakrai², Kenneth Hess³, Chenyue Wendy Hu¹, Alex J. Bisberg¹, Andre Schultz¹, Erik Engquist¹, Li Liu⁴, Xihui Lin⁵, Gregory M. Chen⁵, Honglei Xie⁵, Geoffrey A. M. Hunter⁵, Paul C. Boutros^{5,6}, Oleg Stepanov⁷, DREAM 9 AML-OPC Consortium¹, Thea Norman⁸, Stephen H. Friend⁸, Gustavo Stolovitzky^{2,9}, Steven Kornblau³, Amina A. Qutub^{1*}

1 Rice University, Houston, Texas, United States of America, **2** IBM Computational Biology Center, Yorktown Heights, New York, United States of America, **3** The University of Texas MD Anderson Cancer Center, Houston, Texas, United States of America, **4** Arizona State University, Tempe, Arizona, United States of America, **5** Ontario Institute for Cancer Research, Toronto, Ontario, Canada, **6** Department of Medical Biophysics, University of Toronto, Toronto, Canada, **7** Institute for Systems Biology, Moscow, Russia, **8** Sage Bionetworks, Seattle, Washington, United States of America, **9** Department of Genetics and Genomics Sciences, Icahn School of Medicine at Mount Sinai, New York, New York, United States of America

† Membership of the DREAM 9 AML APC Consortium is provided in the Supporting Information.

* aminaq@rice.edu



OPEN ACCESS

Citation: Noren DP, Long BL, Norel R, Rrhissorakrai K, Hess K, Hu CW, et al. (2016) A Crowdsourcing Approach to Developing and Assessing Prediction Algorithms for AML Prognosis. *PLoS Comput Biol* 12 (6): e1004890. doi:10.1371/journal.pcbi.1004890

Editor: Kai Tan, University of Pennsylvania, UNITED STATES

Received: October 19, 2015

Accepted: March 31, 2016

Published: June 28, 2016

Copyright: © 2016 Noren et al. This is an open access article distributed under the terms of the [Creative Commons Attribution License](https://creativecommons.org/licenses/by/4.0/), which permits unrestricted use, distribution, and reproduction in any medium, provided the original author and source are credited.

Data Availability Statement: Patient data is available at <https://www.synapse.org/#!Synapse:syn2455683/wiki/64007> subject to use agreement. Methods documentation and other information will also be available at the above URL.

Funding: This work was funded in part by the NLM Training Program in Biomedical Informatics T15LM007093-21 (DPN), CPRIT Computational Cancer Training Program (BLL), Sage Bionetworks, MD Anderson Cancer Center Department of Leukemia, and NSF CAREER 1150645 (AAQ). The funders had no role in study design, data collection

Abstract

Acute Myeloid Leukemia (AML) is a fatal hematological cancer. The genetic abnormalities underlying AML are extremely heterogeneous among patients, making prognosis and treatment selection very difficult. While clinical proteomics data has the potential to improve prognosis accuracy, thus far, the quantitative means to do so have yet to be developed. Here we report the results and insights gained from the DREAM 9 Acute Myeloid Prediction Outcome Prediction Challenge (AML-OPC), a crowdsourcing effort designed to promote the development of quantitative methods for AML prognosis prediction. We identify the most accurate and robust models in predicting patient response to therapy, remission duration, and overall survival. We further investigate patient response to therapy, a clinically actionable prediction, and find that patients that are classified as resistant to therapy are harder to predict than responsive patients across the 31 models submitted to the challenge. The top two performing models, which held a high sensitivity to these patients, substantially utilized the proteomics data to make predictions. Using these models, we also identify which signaling proteins were useful in predicting patient therapeutic response.

Author Summary

Acute Myeloid Leukemia (AML) is a hematological cancer with a very low 5-year survival rate. It is a very heterogeneous disease, meaning that the molecular underpinnings that cause AML vary greatly among patients, necessitating the use of precision medicine for

and analysis, decision to publish, or preparation of the manuscript.

Competing Interests: The authors have declared that no competing interests exist.

treatment. While this personalized approach could be greatly improved by the incorporation of high-throughput proteomics data into AML patient prognosis, the quantitative methods to do so are lacking. We held the DREAM 9 AML Outcome Prediction Challenge to foster support, collaboration, and participation from multiple scientific communities in order to solve this problem. The outcome of the challenge yielded several accurate methods (AUROC > 0.78, BAC > 0.69) capable of predicting whether a patient would respond to therapy. Moreover, this study also determined aspects of the methods which enabled accurate predictions, as well as key signaling proteins that were informative to the most accurate models.

Introduction

AML is a potent malignancy of the bone marrow. It is characterized by the production of dysfunctional myeloid cells, incapable of carrying out their normal differentiation into mature blood cells, ultimately leading to hematopoietic insufficiency, infection, hemorrhage, and anemia [1, 2]. The last decade has seen significant revision in the diagnosis and classification of AML. Classification has shifted from a morphology and lineage centered paradigm, described by the French-American-British (FAB) system, to a system which focuses on genetic anomalies, as described by the new World Health Organization (WHO) guidelines [3]. While this includes many of the genetic mutations now recognized to commonly occur in AML [4], recent sequencing efforts [5] have revealed many previously unrecognized mutations in AML which will require further modification of classification schemes. Moreover, genetic events related to epigenetics and non-coding RNAs have yet to be incorporated into classification. Unfortunately, devising an accurate prognosis for AML patients, particularly those with normal cytogenetics, remains very challenging as the combinatorial potential of genetic events makes for tremendous heterogeneity in both classification and outcome interpretation [6]. This can be attributed, in part, to the fact that only a minority of genetic mutations are driver mutations that lead to functional changes in cellular pathways that translate into physiological outcomes.

High-throughput proteomics studies, such as Reverse Phase Proteomic Arrays (RPPA), have the potential to bridge the gap between the underlying genetic alterations and functional cellular changes. Thus far, proteomics has been used successfully to profile AML patients based on alterations in several key signaling pathways, including highly implicated proteins like FLI1 [7] and FOXO3A [8]. However, these studies also confirm that AML remains a very heterogeneous disease, even on the level of protein signal transduction. It is clear that leveraging high-throughput proteomics to improve the accuracy of prognosis for AML patients will require the development of robust quantitative tools. To date, we did not find any studies which address this issue.

The Dialogue for Reverse Engineering Assessment and Methods (DREAM) is a crowdsourcing platform which has accelerated the development of computational tools in the most pertinent areas of biology and medicine, unraveling gene networks [5, 9], predicting drug sensitivity [10], and harnessing predictions to improve prognosis accuracy [11, 12]. Using a challenge based design, DREAM attracts expertise and fosters collaboration across academic fields while providing a mechanism for the robust and unbiased evaluation of computational methods [13–15]. We developed the DREAM Acute Myeloid Leukemia Outcome Prediction Challenge (AML-OPC) following this paradigm.

The DREAM9 AML-OPC was designed to facilitate both the improvement and comprehensive assessment of quantitative AML prognosis methodologies. Challenge participants were

provided access to data from 191 AML patients (the training set) seen at the MD Anderson Cancer Center (Houston, TX), while data from an additional 100 AML (the test set) patients was withheld for model evaluation. We chose Response to Therapy (RT) as the primary clinical endpoint because it is a potentially actionable prognosis criterion. However, since a patient's Remission Duration (RD) and Overall Survival Time (OS) can be informative in planning patient care, these were also included in the challenge objectives.

The DREAM9 AML-OPC included over 270 registered participants and 79 contributing teams, many of which contributed to multiple sub-challenges. Over 60 algorithms were contributed, many of which were refined during the challenge, yielding several innovative and accurate top performing models. We identify these models, test them for robustness, and determine which scoring metrics differentiate the top performers. We also evaluate whether prediction accuracy can be improved by aggregating predictions from the many diverse models we tested. In addition, we evaluate RT predictions over the population of models to determine which outcomes are more difficult to predict accurately. Finally, we investigate the top two performing models to determine the extent their RT predictions were improved by the RPPA data.

Results

Design and implementation of the DREAM 9 AML-OPC

The challenge data consisted of 40 clinical indicators (see [S1 Table](#)) and 231 RPPA measurements ([Fig 1](#)). Three separate sub-challenges were defined to independently address each pertinent aspect of AML prognosis, namely RT for sub-challenge 1 (SC1), RD for sub-challenge 2 (SC2), and the OS for sub-challenge 3 (SC3) ([Fig 1](#)). Two metrics were used to evaluate the performance of models within each sub-challenge. In SC1, RT predictions were contributed as list of confidences indicating the probability that each patient would respond to therapy. The area under the receiver operating characteristic (AUROC) and balanced accuracy (BAC, defined as the average of true positive rate and true negative rate) were selected to assess the RT predictions given their wide use and well documented utility in evaluating classification problems. For SC2 and SC3, RD and OS predictions were submitted as a list of remission or survival times (weeks), respectively, along with a list of corresponding prediction confidences. Both SC2 and SC3 were assessed using the concordance index (CI), which evaluates the ranks of predicted versus actual times when there is censored data and is commonly used in survival analysis. Since the CI considers only the order but not the actual values of the predictions, the Pearson correlation (PC) was also used to evaluate RT and OS.

Evaluating individual and aggregate model performance

The number of teams contributing model predictions increased for each sub-challenge throughout the DREAM9 AML-OPC ([S1A Fig](#)). Participants were allowed to test predictions once per week for a total of 12 weeks ([Fig 2](#)). The same test set was used in the leaderboard phase as well as in the final evaluation. Therefore, predictions were scored on a different sub-sampled (~75%) subset of the 100 patient test set each week to avoid over-fitting. See [Materials and Methods](#) for a more detailed description of the challenge design. Final predictions were collected on the 13th week following the challenge opening. In SC1 ([Fig 2A](#)), the difference in performance between the top RT predictions from the first week and that from the best performing predictions observed during any week of the competition was an increase of 6.21% when evaluated by the AUROC metric alone, 9.20% when evaluated by the BAC alone, and 6.33% when calculating the best average of the two metrics scored by any model. Here, we used the average of both metrics as a summary statistic for the two metrics. The maximum

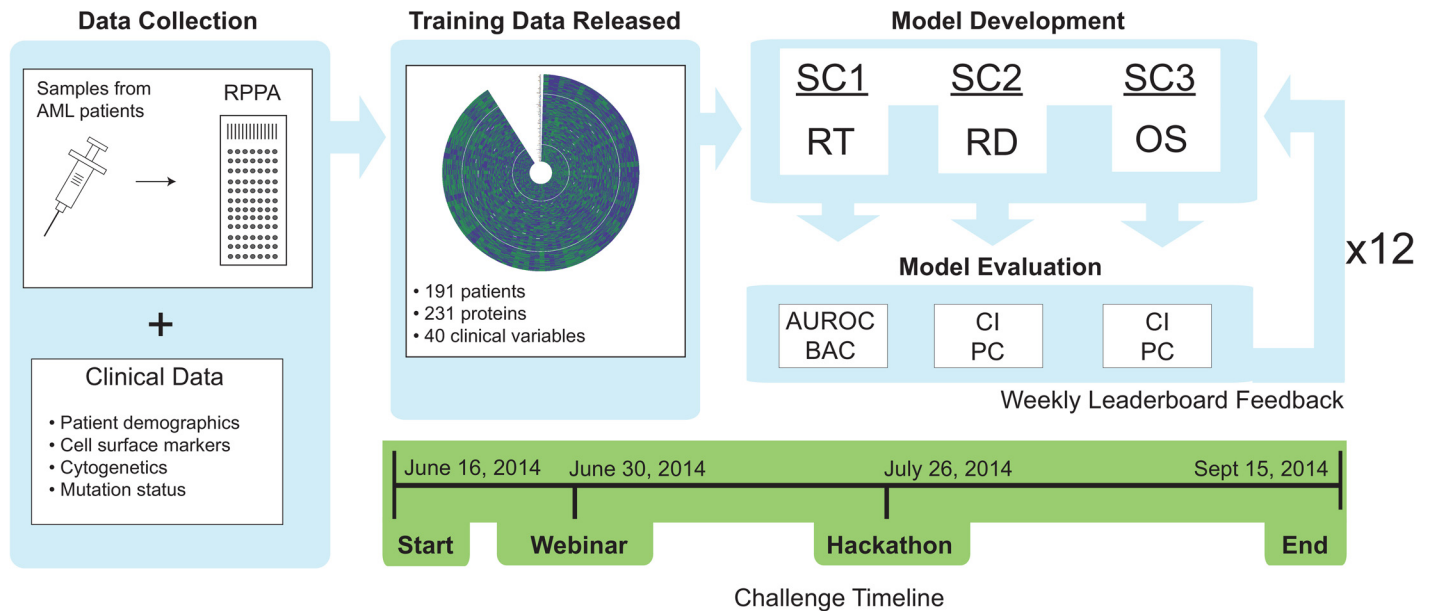


Fig 1. Overview of the DREAM9 AML-OPC data, implementation, and timeline. Samples were collected from 291 patients diagnosed with AML and the levels of 231 signaling proteins were assayed using RPPA. Data was selected from 191 of these patients and released to participants on June 16th 2014 for model training. DREAM9 AML-OPC consisted of 3 subchallenges (SC1, SC2 and SC3) which were evaluated independently on a set of 100 patients (the evaluation was performed on different subsets of 70 patients every week), asking participants to predict either Response to Therapy (RT), Remission Duration (RD), or Overall Survival Time (OS). Participants were given weekly feedback on model performance, which was evaluated using two different metrics for each subchallenge, until September 15th 2014 when the challenge concluded. The metrics were Area Under the Receiver Operating Characteristic (AUROC) curve and Balanced Accuracy (BAC) for SC1, and Concordance Index (CI) and Pearson Correlation (PC) for SC2 and SC3. A hackathon was organized during the Challenge to foster collaboration between participants

doi:10.1371/journal.pcbi.1004890.g001

performance observed during individual weeks is shown in [S1B–S1D Fig](#) (red line). The performance of predictions submitted for the final scoring (week 13) were distributed in a manner distinct from random predictions (see [Fig 2B](#), $p < 0.01$ for AUROC and BAC, Wilcoxon rank sum test), with the top scores being significantly better than random. Note, the median score for each of the previous weeks was also consistently higher than that associated with random predictions ([S1B Fig](#)). The scores from predictions made on the final submission test data (week 13) were frequently lower compared to those made on the training data ([S2 Fig](#)), particularly for the lower ranked models, suggesting that over-fitting was an important factor in determining model performance. For SC1, the top-performing model used a novel evolutionary weighting approach to feature selection (see [S1 Text](#)), yielding a final AUROC score of 0.796 and a BAC of 0.779.

The initial performance of models in predicting RD in SC2 was much lower than observed for RT in SC1, revealing RD predictions were considerably more challenging ([Fig 2C](#)). Even so, generous improvement was seen in both the peak PC and CI scores when comparing the initial scores to the best score observed during the challenge, 47.43% and 11.99% respectively. The highest average metric scores observed during the challenge also showed a marked increase (24.43%). While the distributions of CI and PC scores in the final submission were not as separated from random as the RT predictions ($p < 0.01$ for CI, $p < 0.025$ for PC, Wilcoxon rank sum test) ([Fig 2D](#)), the top scores were higher than expected for random predictions ([S1C Fig](#)). In SC3, OS predictions showed significant improvement when assessing by the CI alone (10.53%), however, the PC showed less increase (~3%) ([Fig 2E](#)). The top average of both metrics showed significant improvement (8.99%) as well. The OS final CI

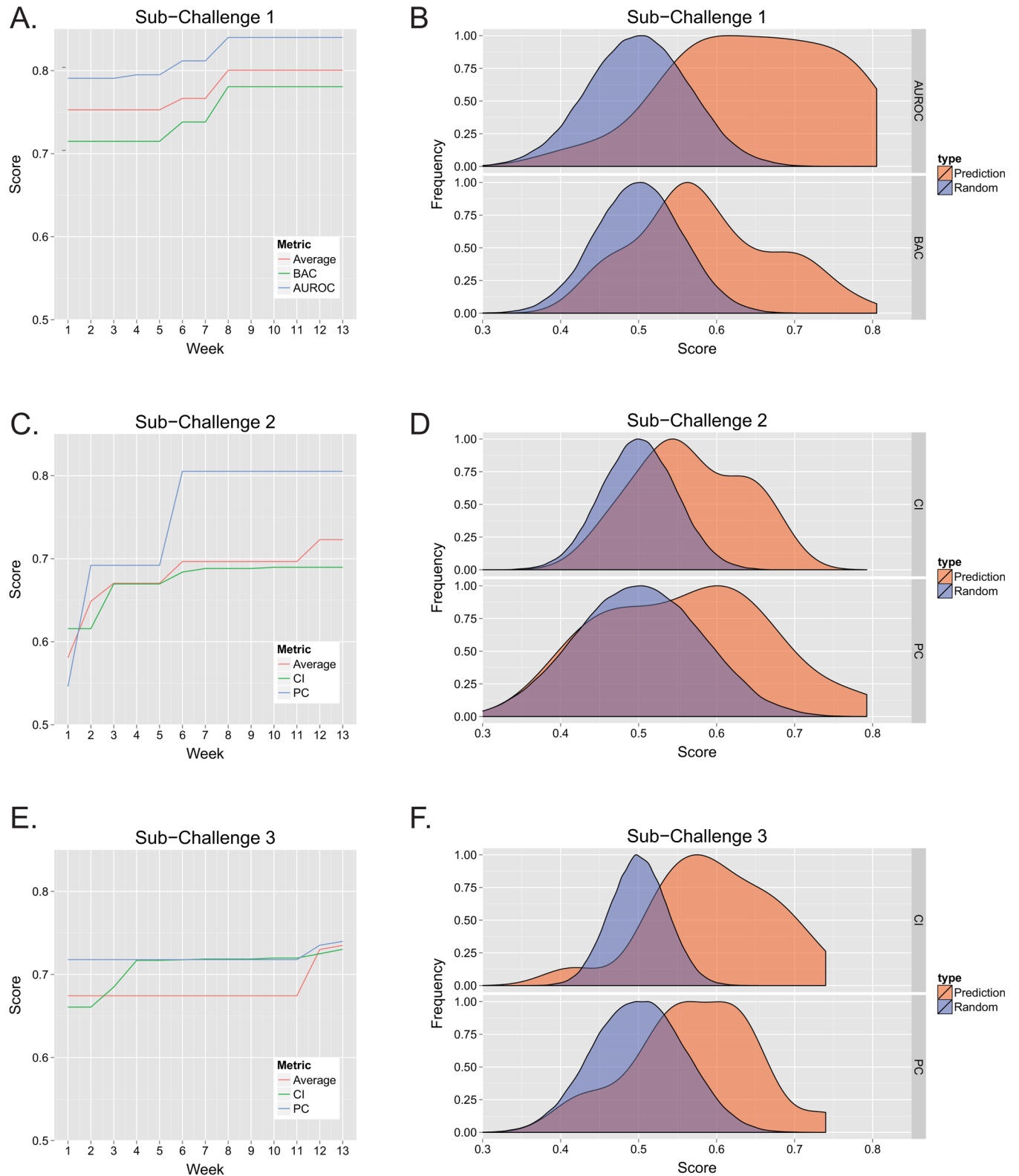


Fig 2. Model performance. The performance of each model was tracked during each week of the challenge. Each sub-challenge was scored using two different metrics. BAC and AUROC were used for SC1, while CI and PC were chosen for SC2 and SC3. The score of the highest performing model was determined each week, either using each metric independently, or by averaging both metrics, and is shown for SC1 (A), SC2 (B), and SC3 (C). Note, if the highest score for any week did not exceed the previous weeks score, the previous score was maintained. The

probability density of the final scores (normalized to a maximum of 1) was also determined and for each metric in SC1 (B), SC2 (D), and SC3 (F). The probability density of the null hypothesis, determined by scoring random predictions, is also indicated.

doi:10.1371/journal.pcbi.1004890.g002

and PC predictions were both significantly shifted from random ($p < 0.01$, Wilcoxon rank sum test) (Fig 2F). The top performing approach for both SC2 and SC3 was developed by a single team and based on Cox Regression (see supplemental text). The model achieved final CI and PC scores of 0.655 and 0.773 for RD predictions in SC2, while obtaining scores of 0.730 and 0.740 for SC3.

A unique facet of community based model development is the ability to examine whether the diverse population of submitted models can be combined to either assure or improve predictive power. Previous DREAM challenges have shown that this approach, often referred to as the “wisdom of crowds”, generates ensemble prediction scores that are comparable in performance, and often times better, than the top performing models [16]. This is particularly useful in real situations when we don’t have a gold standard and therefore we are not certain of which one is the top performing model. Here we aggregate model predictions by calculating the arithmetic mean for the predictions of each model and those models with superior performance. These averaged predictions are then scored to determine aggregate model performance. We tested the performance of aggregate predictions for RT in SC1 and found that the performance increased above the top performing model by 0.04 (~5% improvement based on the average of AUROC and BAC scores) when combining predictions for the top 3 models (Fig 3, leftmost panel). The performance remained higher than the top performing model even after combining the top 5 models and only decreased by 0.11 when combining all 31 models. This score, however, was significantly better than the corresponding score of the 31st ranked model (0.67 compared to 0.42).

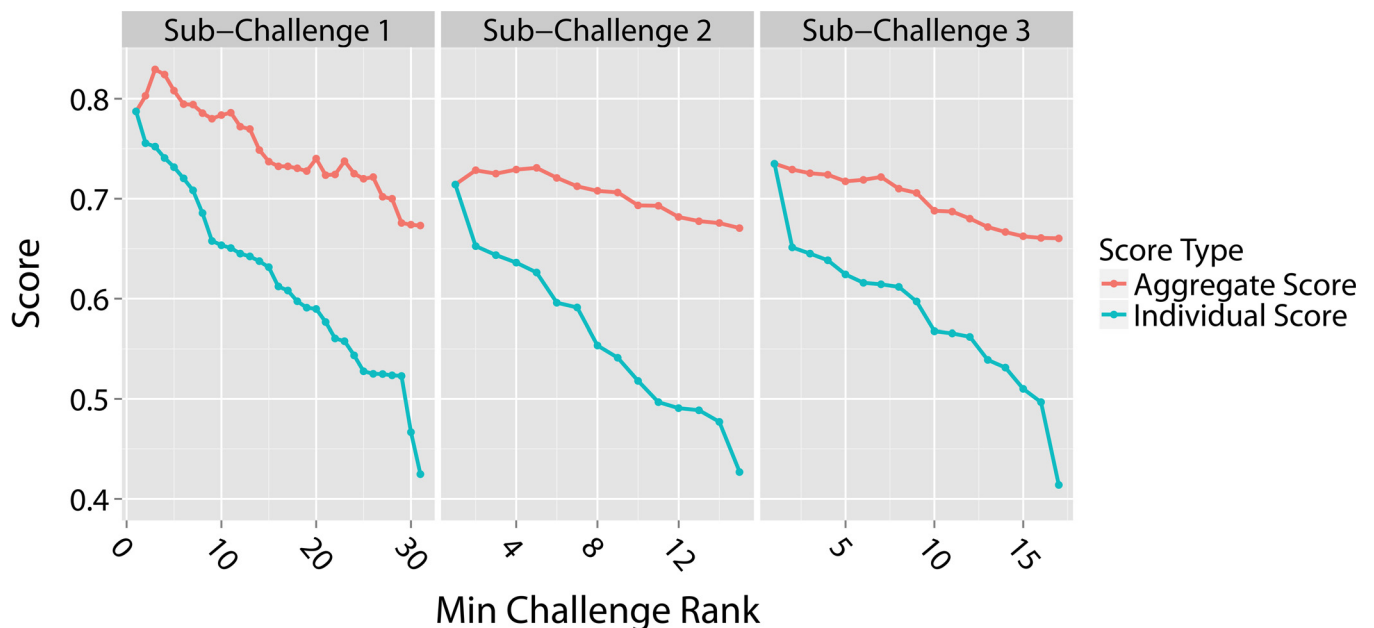


Fig 3. Aggregate and individual model scores. Aggregate scores were determined by averaging the predictions of each model with the predictions from all the models that out-performed it. Model rank is plotted along the x-axis from highest to lowest, with a rank of 1 assigned to the top performing team. Therefore, any given point along the x-axis indicates the minimum rank of the model included in the aggregate score, e.g., a minimum challenge rank of 2 includes predictions from both the rank 2 team and the rank 1 team which out-performed it. The aggregate scores (red lines) were compared to individual team scores (blue lines) for SC1, SC2, and SC3. In each case, the scores reported are the average of the two metrics used for that sub-challenge.

doi:10.1371/journal.pcbi.1004890.g003

Similarly, aggregating RD predictions from the top 5 models in SC2 (Fig 3 –middle panel) also increased performance above the top performing model by 0.02. The aggregate score from all 15 model predictions was only 0.04 less than the top performing score but was 0.24 better than the worst performing model (rank 15). While the aggregate score for OS predictions in SC3 was not higher than the top performing model score (Fig 3, rightmost panel), combining all 17 model predictions results in a prediction that is between the best and second best, only reduced the performance by 0.08 with respect to the top performing team, and resulted in an aggregate score that was 0.25 better than the worst performing model.

Assessing model ranking robustness

A key element in assessing model performance is determining the robustness of the final rankings with respect to perturbations of the test set. We evaluated the stability of the final scores by sampling ~81% of the week 13 test set patients (60 patients out of 74), re-scoring each model, and then repeating 1000 times for each sub-challenge (Fig 4). For SC1, the top

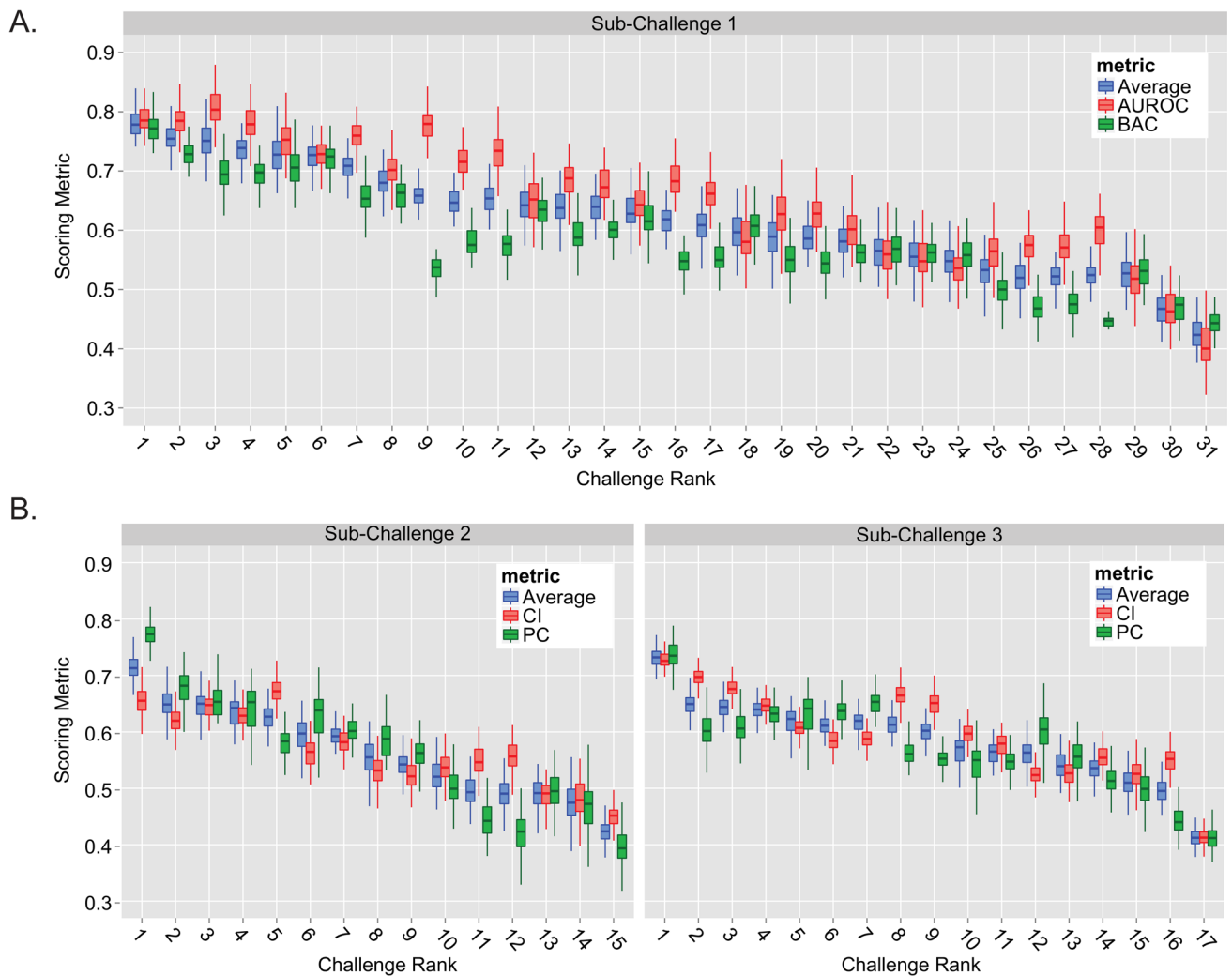


Fig 4. Stability of model performance. Model stability was evaluated for SC1 (A), SC2 (B, left) and SC3 (B, right) by scoring final predictions on 1000 different random subsets of the test set samples (each subset was 60 patients, ~80% of the week 13 test set). The resulting distribution of scores was plotted against each teams overall challenge rank. Note, the center horizontal line of each box indicates the median score. Challenge ranks are ordered from highest to lowest, where a rank of 1 indicates the highest rank.

doi:10.1371/journal.pcbi.1004890.g004

performing model (Challenge Rank = 1) had a combined metric score that was significantly better than all the lower ranked models (average of AUROC and BAC, Bayes Factor (BF) >6.3 with maximum score overlap of 13.7%, see [S3 Fig](#) and [Materials and Methods](#)). When examining each metric separately for the top two teams, we found that the distribution of AUROC scores overlapped 33.8% (BF = 1.95), meaning that the BAC set these models apart (overlap of only 3%, BF = 32.3). As indicated earlier, the same model held the best performance in both SC2 and SC3 ([Fig 4B](#), left and right). In SC2, the combined metric score of the top performing model was significantly better than any of the lower ranked models (maximum overlap of 3.1%, BF = 31.3) due to superior performance when evaluated using the PC metric. In contrast, the top model's resulting CI and PC scores were both superior to the lower ranked models in SC3 (maximum overlap of 3.1%, BF = 31.3).

The role of patient outcome and proteomics data in determining prediction accuracy

We next investigated prediction errors in more detail, focusing on SC1, since RT is a potentially actionable part of prognosis. Specifically, we asked whether either outcome, Complete Remission (CR) or Resistant, was more difficult to predict. Patients in the test set were grouped based on outcome and the predictions from each model were re-scored. The resulting accuracy, taken as the positive prediction value, was distributed distinctly for each outcome ([Fig 5A](#)). The median accuracy for Resistant patients was much lower than CR patients (0.42 vs 0.73, $p < 0.01$, Wilcoxon rank sum test), suggesting they are more difficult to classify ([Fig 5B](#), left). Moreover, 6 of the 7 top performing models achieved accuracies near or above 75% for classifying Resistant patients ([Fig 5B](#), right), well above the median accuracy for that patient group ([Fig 5B](#), left, red box). These same 6 models held accuracies near 70% for CR patients, which were below the median ([Fig 5B](#), left, green box), indicating that accurately classifying Resistant patients set these top models apart. We also examined whether any particular class of learning algorithm was better at predicting the Resistant class of patients, but found a high degree of performance variability amongst implementations that used the same base learners ([S4 Fig](#)).

One of the goals of the DREAM9 AML-OPC was to promote the development of a quantitative method which could utilize the high-throughput RPPA proteomics data to make more accurate prognosis predictions. We examined RPPA data usage for the two highest ranked models from SC1. To do so, we tested each model on scrambled RPPA data, meaning the original trends and RPPA data patterns that were present during model training were removed. Note, scrambled protein data was generated by randomly shuffling patient protein values for each individual protein, meaning the distribution and associated statistics were maintained for each protein. Both models were first tested on data with protein values simultaneously scrambled for all 231 proteins a total of 100 times and scored using the AUROC and BAC metrics. Neither model completely lost predictive power, having median scores of 0.69 and 0.65 for the first and second ranked model, respectively, as evaluated using the average of the AUROC and BAC. However, the resulting scores were much lower when the models made predictions using scrambled data compared to the original scores using the actual RPPA data ([Fig 5C](#)). For both models, the original scores lay at the upper edge of the distribution of scrambled data scores (top 95%). Using the difference between the original scores and the median scrambled RPPA data scores as an estimate, the performance loss was 0.10 (10.7%) and 0.11 (14.6%) for the top and second ranked model ([Fig 5C](#), compare box midline to diamond for the 'average' metric), indicating the RPPA data contributed substantially to each model's predictions.

We next wanted to determine which specific signaling proteins were most pertinent to the performance of the two top models from SC1. To test this, we scrambled the data for each of

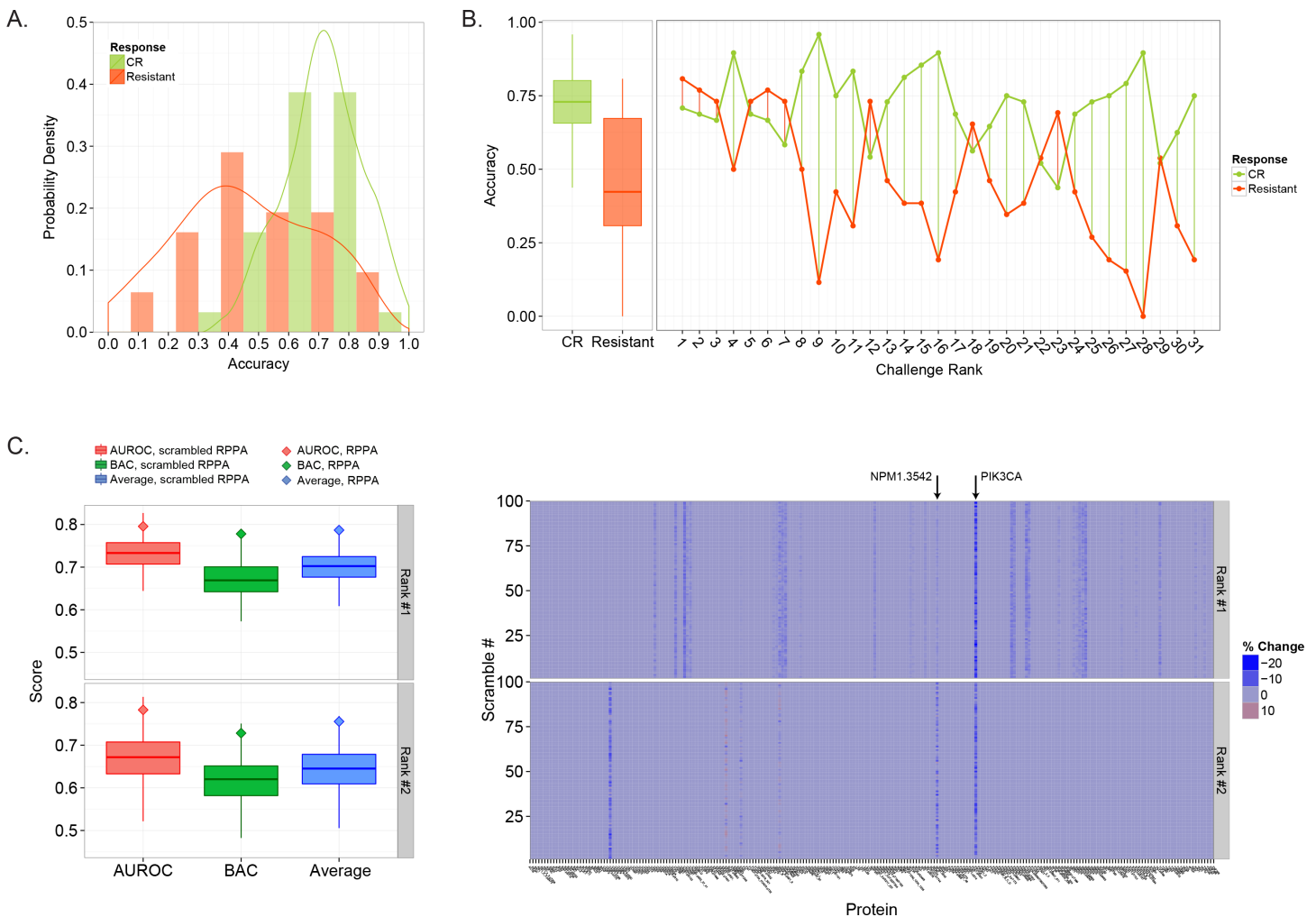


Fig 5. The role of patient outcome and proteomics data in determining prediction accuracy. A) The probability density of prediction accuracy evaluated separately for CR and Resistant patients. (B) Comparison of individual model accuracy for CR and Resistant patients (right) compared to the distribution over the population (left). The midline of the box plot indicated median accuracy while the lower and upper box edge indicated 25th and 75th percentile. (C) The distribution of scores obtained using scrambled RPPA data for the two top performing teams in SC1 (Rank #1 and Rank #2). For each metric, the score obtained using the original RPPA data (not scrambled) is indicated by a diamond. (D) Heat map showing the percent difference in score (average of BAC and AUROC) between predictions obtained using the original RPPA data (not scrambled) and predictions made using data where each protein was scrambled separately over 100 assessments. The y-axis indicates the result for each scrambled protein assessment, 1–100, while the x-axis indicates each protein.

doi:10.1371/journal.pcbi.1004890.g005

the 231 proteins separately over 100 iterations, running each model on a total of 23,100 scrambled data sets. We then evaluated these predictions using a combined metric based on the average of the AUROC and BAC. The percent difference between the original score (unscrambled data) and the score achieved using data with individually scrambled proteins was used to describe the models dependence on each protein (Fig 5D). If a protein was found to influence model performance, data pertaining to that protein was scrambled 10,000 iterations to more accurately assess its impact. For the top performing model (rank #1), randomizing signaling proteins one at a time reduced the model performance in more than 65% of the permutations for 26 proteins (S5A and S5B Fig). For the rank #2 model, 65% or more of the randomizations for each of 4 different proteins decreased model performance (S5C and S5D Fig). Interestingly, perturbing the PIK3CA (Phosphoinositide-3-Kinase, also known as PI3k) signaling protein, an important cell cycle regulator, greatly impacted both models (reducing model performance in

more than 96% of the cases, [Fig 5D](#), compare top and bottom heat map, also [S5 Fig](#)). Indeed, patients that were classified as resistant to therapy were biased towards low levels (<0) of PIK3CA (chi-squared test, $p < 0.00018$, also see [S6 Fig](#)). In addition, the performance of the rank #1 model was also dependent on two other signaling proteins involved in PIK3CA signaling, GSKAB and PTEN. Both models were also dependent on NPM1 (94.36% and 81.43% of permutations reduced performance, rank #1 and rank #2, respectively), a protein which contributes to ribosome assembly and chromatin regulation. Note, both models also utilized several clinical variables ([S7 Fig](#)), including Age, Chemotherapy, and AHD.

Discussion

The absence of new and informative prognostic information has stunted the improvement of AML prognosis accuracy and the advancement of treatment for the last two decades. The DREAM9 AML-OPC gathered researchers from all around the world to address this problem, successfully providing a competitive incentive for progress while maintaining a collaborative environment. This was evident from both the improvement seen in the challenge leaderboards and the wide use of the challenge forums during the competition to convey ideas and voice questions and concerns. In addition, the DREAM9 AML-OPC carried out a webcast “hackathon”, a collaborative tool new to DREAM challenges, where several teams shared insights and local experts presented ideas.

By evaluating the predictions from both good and poor performing models, we were able to use the DREAM9 AML-OPC as a crowdsourcing platform to gain general insight into making more accurate RT predictions. Although many of the models in SC1 were robust, we determined that higher ranked models were distinct in having an elevated and stable median BAC score. In this case, it is likely that the AUROC metric was less sensitive to the class imbalance inherent in the AML data (as discussed in the methods). As this implies the top performers held greater capacity to predict the minority class, i.e., the Resistant patients, we investigated performance on each class in more detail. Indeed, the overall accuracy observed across all the contributed models was lower in predicting the Resistant cases. The top performing models, however, held accuracies well above the median accuracy for the Resistant class, indicating their ability to predict these patients allowed them to obtain higher BAC scores and higher ranks. Accordingly, future efforts in developing RT prognostic models would benefit from improving predictive ability for Resistant patients.

Each sub-challenge resulted in the development of a refined and robust quantitative method to predict a different aspect of patient prognosis. The top model in SC1 used a random forest learning algorithm coupled with a novel form of feature selection called “evolutionary weighting”. Since no general class of learning algorithms could be identified as more accurate in predicting RT, the success of this algorithm likely stems from its implementation and effective feature selection. While the DREAM9 AML-OPC focused on clinically actionable RT predictions, the challenge also resulted in the development of a refined Cox regression model capable of predicting RD and OS. In addition, some participants were also inspired to pursue interesting lines of research beyond the specific aims evaluated by the DREAM9-AML-OPC, for example, exploring characteristics specific to subpopulations of patients [\[17\]](#).

It is important to note, however, potential limitations in our challenge design. The scarcity of AML patient proteomics data available required us to use data from the test set to provide participants with feedback on the weekly leaderboard. This represents an indirect form of information leakage which could potentially lead to the development of over-optimistic models. However, we limited feedback to 12 scorings per participant and used random test set subsamples to minimize potential model overfitting. Moreover, the top model from sub-challenge 1 only submitted to the leaderboard 1 time prior to final judging. Another potential source of

information leakage was the availability of data describing clinical variables and outcomes for a limited number of patients that were used in this study [18]. This data, however, was released many years prior to the DREAM9 AML-OPC and did not have updated patient outcomes. The proteomics data also originated from a different source, and it does not correlate with the data released for the DREAM9 AML-OPC without informed cross normalization. Therefore, it is unlikely this data would be generally informative if participants decided to use it for model training. As a precaution, data pertaining to these patients was excluded from the final model evaluation (week 13) and therefore did not impact the study results.

Beyond developing accurate prognostic models, participants were provided novel clinical RPPA proteomics data and tasked with developing a means to use this information in conjunction with clinical data to improve prognosis accuracy. To our knowledge, the DREAM9 AML-OPC represents the first attempt at both developing a quantitative means to utilize this information and providing a rigorous way to assess the resulting models. Accordingly, we tested the two top performing models for SC1 to see the extent to which their RT predictions depended on the RPPA data. Our findings indicate that the performance of these models was enhanced by using RPPA data, suggesting that clinical proteomics has the potential to become a valuable component to AML prognosis. Moreover, the performance of both models, though derived from very different approaches, was heavily dependent on PI3KCA, suggesting PI3KCA could be a highly informative protein biomarker for predicting AML patient response to therapy. This is congruent with recent studies suggesting PI3KCA mutation is a prognostic factor for AML [19, 20] and that this protein and pathway is potentially an effective therapeutic target [21]. Both models were also dependent on NPM1. The role of NPM1 mutation as a prognostic factor may be unclear. While it is typically associated with higher survival rates in AML [22, 23], a recent study indicates it is not a prognostic factor for AML patients with normal cytogenetics [24]. Our analysis, based on the performance of predictive models that utilize proteomics data rather than genetic data, indicates that NDM1 is an informative feature in predicting AML patient response to therapy.

Materials and Methods

Challenge data

The dataset used for the DREAM 9 AML-OPC consisted of 291 patients seen at the MD Anderson Cancer Center (Houston, TX), for which clinical attributes and RPPA data from bone marrow biopsies was obtained, processed, and normalized as described previously [25–28]. A genetic algorithm was designed to partition the dataset into training and test datasets which have equivalent distributions of clinical and RPPA data. The training set consisted of 191 patients, while the test set held 100 patients. These datasets are available on the [Synapse online repository](#). Note, the clinical outcomes in the overall dataset were imbalanced, with the percent of CR and Resistant patients being approximately 71% and 29% respectively. This ratio was believed to be generally congruent with the overall low survival rate for AML patients and was preserved in both the training and test datasets.

Challenge implementation

The training data was released to participants on June 16th, 2014. Participants were allowed to submit test set predictions for feedback once a week for 13 weeks, from June 23rd to September 8th, 2014 (see [Fig 1](#) for timeline). For each sub-challenge, models were evaluated using two different metrics, and the values for these metrics were posted to the leaderboard each week. Metrics were the AUROC and BAC for SC1, and the CI and PC for both SC2 and SC3. To prevent model over-fitting, 75 out of 100 patients were selected at random for scoring for weeks 1–11.

For weeks 12 and 13, 74 patients were selected to exclude patients for which limited amounts of data might have been available from other sources. Note, SC2 and SC3 required censoring of patients for the purposes of scoring. In SC2, the PC was calculated for RD predictions based solely on patients that responded to therapy and underwent a subsequent relapse. Likewise, for OS predictions in SC3, the PC was determined only for patients that were known to be deceased. For both SC2 and SC3, the CI was determined using right censoring. Final submissions were taken on September 15th, 2014 and scored as described above.

Part of the challenge design included fostering collaboration amongst participants. During the challenge, model scores were posted on a weekly leaderboard so that the progress of every participant was shared throughout the DREAM community. An open “Hackathon” took place on July 26th as part of an effort to foster collaboration in the challenge community. In addition, a community forum was set up so registered participants could ask both technical and administrative questions about the challenge, share ideas, and voice concerns.

Robustness analysis

To check if the ranking resulting from the final model predictions is robust to perturbations of the test set (e.g., removing some of the patients), we re-evaluated each model’s predictions on 1000 sub-samples of the final (week13) test patients. The results of the performance comparison between the model ranked 1st (Rank #1) using the final test set and the models ranked 2nd, 3rd, etc (Rank #2, Rank #3, etc) are shown in [S3 Fig](#). More precisely, if we call ΔM_{1k} the difference in performance metrics of the Rank #1 model (M_1) and model Rank k (M_k), then $\Delta M_{1k} = M_1 - M_k$, under the same sub-sample. [S3 Fig](#) shows the distribution of values of ΔM_{1k} as a function of k. For SC1, the Rank #2 model scores better than Rank #1 in the averaged AUROC and BAC score (that is, ΔM_{12} is negative) in 13.7% of the sub-samples tested. Therefore, while the Rank #1 model does not perform better than the Rank #2 model in all sub-samples, it scores higher with a frequency of 86.3%. If we call $\text{Prob}(M_1 > M_k | D)$ the probability that Model Rank#1 scores higher than model Rank k, and $\text{Prob}(M_k > M_1 | D)$ the probability that model Rank k scores better than model Rank #1 given the data, then the posterior odd ratio is defined as:

$$O^{\text{post}}(1, k) = \text{Prob}(M_1 > M_k | D) / \text{Prob}(M_k > M_1 | D)$$

This ratio measures the fold change of the frequency of model Rank #1 performing higher than model Rank k to the frequency of model Rank k performing better than model Rank #1 given the data at hand. This unprejudiced prior was that model Rank #1 and model Rank k have equal odds of winning. Therefore the prior odds ratio is given by:

$$O^{\text{prior}}(1, k) = \text{Prob}(M_1 > M_k) / \text{Prob}(M_k > M_1) = 1$$

The Bayes Factor K is defined as the ratio between posterior odds and prior odds ratios:

$$\text{BF}(1, k) = O^{\text{post}}(1, k) / O^{\text{prior}}(1, k)$$

For hypothesis testing, where the conventional statistical significance is given by p-values < 0.05, well established guidelines for the interpretation of Bayes Factors [29] suggest that $\text{BF}(1,k) > 3, 20$ and 150 gives positive, strong, and very strong evidence in favor of $M_1 > M_k$.

For sub-challenges 1, 2 and 3 we have that $\text{BF}(1,2)$ is equal to 6.3, 332 and >999, indicating a robustness of the relative ranking between Rank #1 and Rank #2 models in the Challenge. This robustness holds for all metrics and all sub-challenges, except for metric AUROC in SC1, for which model Rank #1 cannot be considered to be better than model Rank #2, #3 or #4.

Assessing the importance of the RPPA data

Use of the RPPA data was determined for the two top scoring models in SC1 by scrambling the protein data, making predictions with the previously trained models, and comparing the scores to those from the original predictions that were made with the unscrambled RPPA data. The data was scrambled by randomly shuffling the values for each individual protein across the 100 patients in the test dataset. In this way, the statistical properties, e.g., the mean, variance, range, etc, were preserved for every protein. All proteins in the dataset were scrambled in this manner for each assessment and a total of 100 assessments were conducted. Note, each model was scored using the final (week 13) test dataset (74 patients). Reduction in model performance was measured by the percentage of scores that were lower than the original predictions, i.e., dividing the number of scores that were less than the original (unscrambled) by the total number of scores from scrambled RPPA assessments.

The procedure to determine which specific proteins were informative to the two top performing models was the same as described above, with the exception that only 1 protein was scrambled for each of the assessments. Again, this was repeated 100 times, making a total of 23,100 scrambled assessments for the 231 proteins. To more accurately determine the percentage of perturbations that decreased model performance, an additional 10,000 assessments were performed for proteins that altered model performance under the initial 100 assessments.

Statistical computing

Challenge results were analyzed using the statistical computing language R [30]. Figure plots were developed using the package ggplot2 [31].

Supporting Information

S1 Fig. Summary of team participation and performance each week. (A) The number of teams participating in each sub-challenge each week. (B-D) Box plots comparing the distribution of scores each week with scores generated from random predictions for each sub-challenge. The red line indicates the maximum score seen for each week.

(TIF)

S2 Fig. Comparison of model performance on training and test datasets. Model performance was evaluated on the week 13 test data (red) and training data (blue). (A) Performance for SC1 was determined using the AUROC (top) and BAC (bottom) scores (B) Performance for SC2 was determined using the CI (top) and PC (bottom) scores. (C) Performance for SC3 was determined using the CI (top) and PC (bottom) scores.

(TIF)

S3 Fig. Paired differences for stability analysis of model performance. Model stability was evaluated by scoring final predictions on 1000 different random subsets of the week 13 test set patients (81%). For each specific subset, the difference between the Rank #1 model score and each lower ranking model was determined. Positive differences are indicated by blue points while negative differences are shown in red. The text above each set of points indicates the fraction of scores in which a lower ranking model outperformed the rank #1 model.

(TIF)

S4 Fig. Accuracy in predicting CR and Resistant patients for different machine learning methods. Each model was classified by its base machine learning method as documented in the write-ups submitted by each participant. The accuracy in predicting both CR and Resistant patients, taken as the positive predictive value, was then determined for each model. Note,

“Meta” refers to models that used a combination of multiple different machine learning approaches, while other refers to approaches that did not use machine learning methods. These methods included various implementations of descriptive statistics, probability analysis, and sparse matrix analysis.

(TIF)

S5 Fig. Proteins found to impact the performance of the Rank #1 and Rank #2 models in SC1.

(A) Box plots comparing the distribution of scores obtained by scrambling individual protein data over 100 assessments (see [methods](#)) for the Rank #1 model. Each box centerline indicates the median score while the upper and lower box borders indicate the 25th and 75th percentile respectively. (B) Table showing the percentage of randomizations that yielded reduced scores with respect to the original (unscrambled) RPPA data for the Rank #1 model. (C) Box plots, as described in A, showing the distribution of scores obtained by scrambling individual protein data over 100 assessments for the Rank #2 model. (D) Table showing the percentage of randomizations that yielded reduced scores with respect to the original (unscrambled) RPPA data for the Rank #2 model.

(TIF)

S6 Fig. Distribution of PIK3CA levels for patients classified as CR or Resistant. A histogram showing the number of patients for different levels of PIK3CA. The vertical centerline at 0 denotes the boundary between low and high PIK3CA levels.

(TIF)

S7 Fig. Clinical variables found to impact the performance of the Rank #1 and Rank #2 models in SC1.

(A) Heat map showing the percent difference in score (average of BAC and AUROC) between predictions obtained using the original clinical variables (not scrambled) and predictions made using data where each clinical variable was scrambled separately over 100 assessments. The y-axis indicates the result for each scrambled assessment, 1–100, while the x-axis indicates each clinical variable. (B) Box plots comparing the distribution of scores obtained by scrambling data from individual clinical variables over 100 assessments (see [Methods](#)) for the Rank 1 model. Each box centerline indicates the median score while the upper and lower box borders indicate the 25th and 75th percentile respectively. (C) Table showing the percentage of perturbations that resulted in reduced scores after scrambling each individual clinical variable for the Rank #1 model. (D) Box plots, as described in B, showing the distribution of scores obtained by scrambling data pertaining to individual clinical variables over 100 assessments for the Rank #2 model. (E) Table showing the percentage of perturbations that resulted in reduced scores after scrambling each individual clinical variable for the Rank #2 model.

(TIF)

S1 Table. Clinical covariates included as data in the DREAM 9 AML-OPC Challenge.

(TIF)

S1 Text. Participant description of best performing methods. The description of the best performing methods, as provided by participants, for SC1, SC2, and SC3.

(PDF)

S2 Text. Membership list for the DREAM 9 AML-OPC consortium.

(PDF)

Acknowledgments

We would like to thank Dr. Gordon Mills (MD Anderson Cancer Center, University of Texas), Dr. Elihu Estey (Fred Hutchinson Cancer Center, University of Washington), and Dr. Jerald

Radish (Fred Hutchinson Cancer Center, University of Washington) for their insight and advise. We also thank Bruce Hoff (Sage Bionetworks) and Jay Hodgson (Sage Bionetworks) for technical support during the DREAM challenge. We thank the Ken Kennedy Institute for Information Technology for their computing support, and DiBS for supporting visualization of the open data.

Author Contributions

Conceived and designed the experiments: DPN AAQ SK GS RN BLL TN SHF KR. Performed the experiments: DPN BLL LL OS XL GMC HX GAMH PCB KH. Analyzed the data: DPN BLL RN. Contributed reagents/materials/analysis tools: CWH AJB AS SHF EE. Wrote the paper: DPN AAQ GS.

References

1. Lowenberg B, Downing JR, Burnett A. Acute myeloid leukemia. *N Engl J Med.* 1999; 341(14):1051–62. Epub 1999/09/30. PMID: [10502596](#)
2. Estey E, Dohner H. Acute myeloid leukaemia. *Lancet.* 2006; 368(9550):1894–907. Epub 2006/11/28. PMID: [17126723](#)
3. Vardiman JW, Thiele J, Arber DA, Brunning RD, Borowitz MJ, Porwit A, et al. The 2008 revision of the World Health Organization (WHO) classification of myeloid neoplasms and acute leukemia: rationale and important changes. *Blood.* 2009; 114(5):937–51. Epub 2009/04/10. doi: [10.1182/blood-2009-03-209262](#) PMID: [19357394](#)
4. Dohner H, Estey EH, Amadori S, Appelbaum FR, Buchner T, Burnett AK, et al. Diagnosis and management of acute myeloid leukemia in adults: recommendations from an international expert panel, on behalf of the European LeukemiaNet. *Blood.* 115(3):453–74. Epub 2009/11/03. doi: [10.1182/blood-2009-07-235358](#) PMID: [19880497](#)
5. Marbach D, Prill RJ, Schaffter T, Mattiussi C, Floreano D, Stolovitzky G. Revealing strengths and weaknesses of methods for gene network inference. *Proc Natl Acad Sci U S A.* 107(14):6286–91. Epub 2010/03/24. doi: [10.1073/pnas.0913357107](#) PMID: [20308593](#)
6. Martelli MP, Sportoletti P, Tiacci E, Martelli MF, Falini B. Mutational landscape of AML with normal cytogenetics: biological and clinical implications. *Blood Rev.* 27(1):13–22. Epub 2012/12/25. doi: [10.1016/j.blre.2012.11.001](#) PMID: [23261068](#)
7. Kornblau SM, Qiu YH, Zhang N, Singh N, Faderl S, Ferrajoli A, et al. Abnormal expression of FLI1 protein is an adverse prognostic factor in acute myeloid leukemia. *Blood.* 118(20):5604–12. Epub 2011/09/16. doi: [10.1182/blood-2011-04-348052](#) PMID: [21917756](#)
8. Kornblau SM, Singh N, Qiu Y, Chen W, Zhang N, Coombes KR. Highly phosphorylated FOXO3A is an adverse prognostic factor in acute myeloid leukemia. *Clin Cancer Res.* 16(6):1865–74. Epub 2010/03/11. doi: [10.1158/1078-0432.CCR-09-2551](#) PMID: [20215543](#)
9. Meyer P, Cokelaer T, Chandran D, Kim KH, Loh PR, Tucker G, et al. Network topology and parameter estimation: from experimental design methods to gene regulatory network kinetics using a community based approach. *BMC Syst Biol.* 8:13. Epub 2014/02/11. doi: [10.1186/1752-0509-8-13](#) PMID: [24507381](#)
10. Costello JC, Heiser LM, Georgii E, Gonen M, Menden MP, Wang NJ, et al. A community effort to assess and improve drug sensitivity prediction algorithms. *Nat Biotechnol.* 32(12):1202–12. Epub 2014/06/02. doi: [10.1038/nbt.2877](#) PMID: [24880487](#)
11. Margolin AA, Bilal E, Huang E, Norman TC, Ottestad L, Mecham BH, et al. Systematic analysis of challenge-driven improvements in molecular prognostic models for breast cancer. *Sci Transl Med.* 5(181):181re1. Epub 2013/04/19. doi: [10.1126/scitranslmed.3006112](#) PMID: [23596205](#)
12. Kuffner R, Zach N, Norel R, Hawe J, Schoenfeld D, Wang L, et al. Crowdsourced analysis of clinical trial data to predict amyotrophic lateral sclerosis progression. *Nat Biotechnol.* 33(1):51–7. Epub 2014/11/05. doi: [10.1038/nbt.3051](#) PMID: [25362243](#)
13. Prill RJ, Marbach D, Saez-Rodriguez J, Sorger PK, Alexopoulos LG, Xue X, et al. Towards a rigorous assessment of systems biology models: the DREAM3 challenges. *PLoS One.* 5(2):e9202. Epub 2010/02/27. doi: [10.1371/journal.pone.0009202](#) PMID: [20186320](#)
14. Norel R, Rice JJ, Stolovitzky G. The self-assessment trap: can we all be better than average? *Mol Syst Biol.* 7:537. Epub 2011/10/13. doi: [10.1038/msb.2011.70](#) PMID: [21988833](#)

15. Boutros PC, Margolin AA, Stuart JM, Califano A, Stolovitzky G. Toward better benchmarking: challenge-based methods assessment in cancer genomics. *Genome Biol.* 15(9):462. Epub 2014/10/16. doi: [10.1186/s13059-014-0462-7](https://doi.org/10.1186/s13059-014-0462-7) PMID: [25314947](https://pubmed.ncbi.nlm.nih.gov/25314947/)
16. Marbach D, Costello JC, Kuffner R, Vega NM, Prill RJ, Camacho DM, et al. Wisdom of crowds for robust gene network inference. *Nat Methods.* 9(8):796–804. Epub 2012/07/17. doi: [10.1038/nmeth.2016](https://doi.org/10.1038/nmeth.2016) PMID: [22796662](https://pubmed.ncbi.nlm.nih.gov/22796662/)
17. Contributed Methods. A description of many of the contributed methods can be found at the Synapse website hosted by Sage Bionetworks under the “write-up” heading of the [final leaderboard](https://www.synapse.org/) <<https://www.synapse.org/>>. In particular, a novel method using multivariate features to identify a small cohort of patients who respond to therapy is discussed by Team Attractor Metagenes <<https://www.synapse.org/#!Synapse:syn2699097/wiki/68362>>].
18. Kornblau SM, Tibes R, Qiu YH, Chen W, Kantarjian HM, Andreeff M, et al. Functional proteomic profiling of AML predicts response and survival. *Blood.* 2009; 113(1):154–64. Epub 2008/10/09. doi: [10.1182/blood-2007-10-119438](https://doi.org/10.1182/blood-2007-10-119438) PMID: [18840713](https://pubmed.ncbi.nlm.nih.gov/18840713/)
19. Park S, Chapuis N, Tamburini J, Bardet V, Cornillet-Lefebvre P, Willems L, et al. Role of the PI3K/AKT and mTOR signaling pathways in acute myeloid leukemia. *Haematologica.* 95(5):819–28. Epub 2009/12/03. doi: [10.3324/haematol.2009.013797](https://doi.org/10.3324/haematol.2009.013797) PMID: [19951971](https://pubmed.ncbi.nlm.nih.gov/19951971/)
20. Tamburini J, Elie C, Bardet V, Chapuis N, Park S, Broet P, et al. Constitutive phosphoinositide 3-kinase/Akt activation represents a favorable prognostic factor in de novo acute myelogenous leukemia patients. *Blood.* 2007; 110(3):1025–8. Epub 2007/04/12. PMID: [17426258](https://pubmed.ncbi.nlm.nih.gov/17426258/)
21. Thomas D, Powell JA, Vergez F, Segal DH, Nguyen NY, Baker A, et al. Targeting acute myeloid leukemia by dual inhibition of PI3K signaling and Cdk9-mediated Mcl-1 transcription. *Blood.* 122(5):738–48. Epub 2013/06/19. doi: [10.1182/blood-2012-08-447441](https://doi.org/10.1182/blood-2012-08-447441) PMID: [23775716](https://pubmed.ncbi.nlm.nih.gov/23775716/)
22. Falini B, Mecucci C, Tiacci E, Alcalay M, Rosati R, Pasqualucci L, et al. Cytoplasmic nucleophosmin in acute myelogenous leukemia with a normal karyotype. *N Engl J Med.* 2005; 352(3):254–66. Epub 2005/01/22. PMID: [15659725](https://pubmed.ncbi.nlm.nih.gov/15659725/)
23. Liu Y, He P, Liu F, Shi L, Zhu H, Zhao J, et al. Prognostic significance of NPM1 mutations in acute myeloid leukemia: A meta-analysis. *Mol Clin Oncol.* 2(2):275–81. Epub 2014/03/22. PMID: [24649346](https://pubmed.ncbi.nlm.nih.gov/24649346/)
24. Pastore F, Greif PA, Schneider S, Ksienzyk B, Mellert G, Zellmeier E, et al. The NPM1 mutation type has no impact on survival in cytogenetically normal AML. *PLoS One.* 9(10):e109759. Epub 2014/10/10. doi: [10.1371/journal.pone.0109759](https://doi.org/10.1371/journal.pone.0109759) PMID: [25299584](https://pubmed.ncbi.nlm.nih.gov/25299584/)
25. Neeley ES, Kornblau SM, Coombes KR, Baggerly KA. Variable slope normalization of reverse phase protein arrays. *Bioinformatics.* 2009; 25(11):1384–9. Epub 2009/04/02. doi: [10.1093/bioinformatics/btp174](https://doi.org/10.1093/bioinformatics/btp174) PMID: [19336447](https://pubmed.ncbi.nlm.nih.gov/19336447/)
26. Hu J, He X, Baggerly KA, Coombes KR, Hennessy BT, Mills GB. Non-parametric quantification of protein lysate arrays. *Bioinformatics.* 2007; 23(15):1986–94. Epub 2007/06/30. PMID: [17599930](https://pubmed.ncbi.nlm.nih.gov/17599930/)
27. Tibes R, Qiu Y, Lu Y, Hennessy B, Andreeff M, Mills GB, et al. Reverse phase protein array: validation of a novel proteomic technology and utility for analysis of primary leukemia specimens and hematopoietic stem cells. *Mol Cancer Ther.* 2006; 5(10):2512–21. Epub 2006/10/17. PMID: [17041095](https://pubmed.ncbi.nlm.nih.gov/17041095/)
28. Neeley ES, Baggerly KA, Kornblau SM. Surface Adjustment of Reverse Phase Protein Arrays using Positive Control Spots. *Cancer Inform.* 2012; 11:77–86. Epub 2012/05/03. doi: [10.4137/CIN.S9055](https://doi.org/10.4137/CIN.S9055) PMID: [22550399](https://pubmed.ncbi.nlm.nih.gov/22550399/)
29. Kass RE, Raftery AE. Bayes Factors. *Journal of the American Statistical Association.* 1995; 90(430):773–95.
30. Team RC. R: A Language and Environment for Statistical Computing. Vienna, AustriaVienna, Austria.
31. Wickham H. ggplot2: elegant graphics for data analysis: Springer New York; 2009.

Sub-challenge #1, Rank #1 Model

Title

Author: Li Liu

Affiliation: Arizona State University

Email: leew369@gmail.com

Summary Sentence

Features are weighted based on their evolutionary conservations and t test p-values during the feature selection step, while un-weighted selected features are used in an ensemble of random forest modeling.

Background/Introduction

From the perspective of long-term evolutionary history, cancer genes are highly conserved among species [1]. In the same vein, cancer driver mutations are almost always found at evolutionarily conserved positions that lead to deleterious loss- or gain- of functions [2]. Based on these observations, it is reasonable to infer that changes of expression levels, another mechanism of functional regulation, will have more profound impact if they involve highly conserved proteins, as compared to less conserved proteins. In fact, studies have shown that expression level is a strong correlate of evolutionary conservation [3]. Therefore, I designed a weighting scheme to improve the RPPA data in predicting AML remissions [4].

The basic idea is to give higher weights to conserved proteins and lower weights to variable proteins. Conservation of a protein can be calculated using evolutionary approaches (see Method). Furthermore, differentially expressed proteins shall be given higher weights, which can be represented by p-values from student t tests. A combination of these two measurements gives rise to the final weights.

After each feature is transformed using its specific weight, feature selection is performed. This process will favor features that are more evolutionarily conserved and more differentially distributed between two classes. In the classification step, models are built upon selected but un-weighted features.

Methods

Preprocessing data: Categorical features were coded using dummy variables. For each feature, the raw values were transformed to z scores, which had mean of 0 and standard deviation of 1. Missing values were imputed by random sampling. Four features with low information content (entropy<0.05) were removed. Since no two features shared > 95% correlation, all of them were treated as independent features.

Calculating weights: For each protein, the multiple sequence alignments of 46 vertebrates (Figure 1) were downloaded from the UCSC Genome Browser [5]. At a given position, the evolutionary rate (r) is calculated as the number of substitutions per billion years [6]. The conservation of a protein is measured as the average of r over all positions. Because high evolutionary rate indicates low conservation, the reciprocal of evolutionary rate ($1/r$) is used as the evolutionary weight (WE) for each protein. For clinical features, the evolutionary weights were set to be the maximum of WE . For each feature, a two-side student t test was performed. P-values were transformed via negative logarithm ($-\log(P)$) and used as the differential weight (WD). For each feature i , the final weight was the sum of evolutionary and differential weights ($W_i = WE_i + WD_i$).

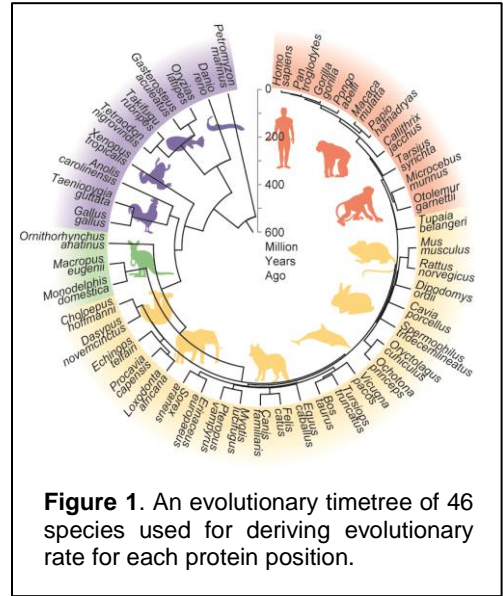


Figure 1. An evolutionary timetree of 46 species used for deriving evolutionary rate for each protein position.

Constructing ensemble models: Because the training data are highly unbalanced, we employed an ensemble approach that constructs multiple classification models using balanced subsamples [7]. Specifically, a subset of 50 samples was randomly selected from each class (CR labeled as 1, Resistant labeled as 0). This number was determined as 90% of samples in the under-represented resistant class. In the feature selection step, values of each feature were multiplied by their corresponding weights. Then, stability selection [8] with sparse logistic regression was performed, as implemented in the SLEP package [9]. During stability selection, bootstrapping was used to identify features that were consistently selected among multiple runs with a wide range of regularization parameters. Features identified in >50% of bootstrapping runs were selected. In the classification step, selected features with un-weighted values were used to construct a random forest model with 50 trees. The above procedure was repeated 100 times, which produced an ensemble of 100 random forest models.

Making predictions: For each sample in the testing dataset, we derived 100 predictions, one from each random forest model. The confidence score equals the percentage of models that predict the sample as CR.

Multiple submissions: In total, I submitted the predictions twice. The first submission was derived from an ensemble of 30 random forest models. The final submission was from 100 models. The correlation between these two submissions was very high (97%). It will be interesting to compare predictions with and without using the weighting scheme. Unfortunately, because I joined the project only two weeks before its closing date, I missed the opportunity to test different models.

Conclusion/Discussion

Because I only have one submission scored (submission ID: 2669636), it is hard to assess the contribution of evolutionary and differential weights to the prediction accuracy. However, this single submission achieved BAC score of 0.7283 and AUROC score of 0.7704, which had an overall rank of #1 in the week of September 8th. Therefore, the performance of this approach is at least comparable to other top-ranked methods.

Meanwhile, I am aware that team YL also participated in the Challenge. The lead of team YL, Dr. Ye, is a close collaborator of mine. In the classification step, both of our teams used an ensemble of random forest models. However, team YL took a different strategy in the feature selection step. Once the models from our two teams are disclosed, we will be able to infer the contribution of evolutionary and differential weights to the prediction accuracy. However, the ultimate evaluation will come from more systematic comparisons.

Author Statement

I thank Dr. Ye for inviting me to the Challenge, and giving advices in using the SLEP package.

References

1. Goymer P. (2007) Genetics: Conserved by evolution, but altered in cancer. *Nature Reviews Cancer*. 7:812-813.
2. Kumar S, Dudley JT, Filipski A, Liu L. (2011) Phylomedicine: an evolutionary telescope to explore and diagnose the universe of disease mutations. *Trends in Genetics*. 27(9):377-86.
3. Drummond DA, Raval A, Wilke CO. (2006) A single determinant dominates the rate of yeast protein evolution. *Molecular Biology and Evolution*. 23(2):327-37.
4. DREAM Acute Myeloid Leukemia Outcome Prediction Challenge (syn2455683)
5. Rosenbloom KR, Sloan CA, Malladi VS, Dreszer TR, Learned K, Kirkup VM, et al. (2013) ENCODE data in the UCSC Genome Browser: year 5 update. *Nucleic acids research*. 41:D56-63.
6. Kumar S, Sanderford M, Gray VE, Ye J, Liu L. (2012) Evolutionary Diagnosis Method for Variants in Personal Exomes. *Nature Methods*. 9(9):855-6
7. Dubey R, Zhou J, Wang Y, Thompson PM, Ye J (2014) Analysis of sampling techniques for imbalanced data: An n = 648 ADNI study. *Neuroimage*. 15;87:220-41
8. Meinshausen N, Buhlmann P. (2010) Stability selection. *Journal of the Royal Statistical Society: Series B*. 72:417-73.
9. Liu J, Ji S, Ye J. (2009) SLEP: Sparse Learning with Efficient Projections. Arizona State University. <http://www.public.asu.edu/~jye02/Software/SLEP>

Sub-challenge #1, Rank #2 Model

Introduction

My approach was to develop a General Linear Model (GLM) class of base learner, using bootstrapping for model training and repeated random sub-sampling for validation. The use of a GLM framework was motivated by both its effectiveness and easy interpretation. Since the amount of data available was limited, I used bootstrapping for parameter selection and validation of my model.

I approached this problem without the use of any prior biological or medical knowledge, allowing the model to discern which features and feature combinations are most informative. In particular, I was interested in testing combinations and interactions of features using both RPPA data and clinical data.

Method

To pre-process the data, I first excluded clinical covariates that contained many "NA" values. While that could lead to information loss, I decided to use only parameters that contain sufficient information.

Model construction consists of several steps:

- 1) I created a list with all parameters and all possible linear combination of 2 and 3 parameters.
- 2) I checked the prediction ability for those models. I found that even if model consisting of one parameter has low prediction ability, some combination with that parameter could still have good predictive ability.
- 3) For each model, I split the initial data set into 2 parts and increased number of patients with bootstrapping. In general I had increased number of patients with CR and Resistant status to 1000 each by sampling with replacement. I repeated this step 1000 times and calculated the median BAC score for each model.
- 4) Next I sorted all the models by BAC score and selected all models with scores more than 0.5.
- 5) Finally, I found the best combinations of features from models with high scores. I started from best model and added successive models with lower scores. Analysis of predictive power was the same. If new model has higher score it becomes best model.

Conclusion

Using GLM method with multiple linear combinations yielded favorable results with the benefit of having a final model that is easy to interpret. One disadvantage was that this method required a great deals of computational time and power.

Sub-challenge #2, Rank #1 Model

A bagged semi-parametric model for predicting remission duration in AML sub-challenge 2

Xihui Lin : Eric.Lin@oicr.on.ca
Gregory M. Chen : gregorymchen@gmail.com
Honglei Xie : xhonglei2007@gmail.com
Geoffrey A. M. Hunter : Geoffrey.Hunter@oicr.on.ca
Paul C. Boutros : Paul.Boutros@oicr.on.ca

October 13, 2015

Summary

We implemented a bootstrap aggregated (bagged) Cox-like semi-parametric model with carefully selected predictors as a predictive model for remission duration for the AML sub-challenge 2.

1 Introduction

Why a bagged semi-parametric model

- The performance of the benchmark model using a standard Cox model with five selected clinical predictors is comparable to the top models on the leaderboard and better than our previous models such as survival random forests, boosted quantile regression, and weighted linear model.
- A native average over all submissions in sub-challenge 2 & 3 performs surprisingly well on the leaderboard, so we reasoned that averaging (via bagging) would be a viable strategy to reduce the variance.

Variable selection

- The benchmark model, with an impressive performance, uses only five selected clinical variables.
- From our work on sub-challenge 1, our model performance decreased whenever we incorporated one or more of the protein data, so we omitted this data from our models for sub-challenge 2 & 3 model.
- Based on these observations we started with the selected five clinical variables, i.e., *Age.at.Dx*, *Chemo.Simplest*, *HGB*, *ALBUMIN* and *cyto.cat*.

Missing values

Since there are only a few missing values of the selected variables in the training and testing sets, we simply replace them by the medians and modes for continuous and discrete variables respectively.

2 Methods

2.1 Preprocessing: re-categorizing ‘cyto.cat’

This part was done and shown in the supplement for sub-challenge 3, using overall survival time as outcome. We didn’t re-do the analysis for remission duration as the results were shown in [1] to be similar. The re-categorized *cyto.cat* is shown in Table 1.

Risk Category	Abnormality
High	'-5,-7', '-5,-7,+8', '-7', '-7,+8'
Intermediate (baseline)	'-5', '11q23', '8', 'IM', 'Misc', 't6;9', 't9;22', 'inv9'
Intermediate-low	'diploid'
Lower	'inv16', 't8;21'

Table 1: New cytogenetics categories.

2.2 Model

An appropriate model for bagging is one that should be unbiased with high variation. For this purpose, we added some ‘frailty’ terms (inspired by frailty in survival model and the positivity of the selected continuous variables) to the standard Cox proportional hazard model as

$$\lambda(t|x, z) = \lambda_0(t)x^\alpha \exp(x\beta + z\gamma) \quad (1)$$

where x is a vector of positive continuous variates and z is a vector of discrete variables, and

$$x^\alpha := (x_1, \dots, x_k)^{(\alpha_1, \dots, \alpha_k)} := \prod_{i=1}^k x_i^{\alpha_i}.$$

Indeed, equation (1) is equivalent to

$$\lambda(t|x, z) = \lambda_0(t) \exp((\log x)\alpha + x\beta + z\gamma). \quad (2)$$

We draw $B = 1000$ bootstrap samples. With each bootstrap sample, model (2) is fitted with R function *coxph*(R-3.1.1, survival-2.37-7). The final prediction from this bagged model is a simple average over all $B = 1000$ base models. Out-of-bag (OOB) samples are used to assess the performance, which typically slightly underestimates the performance. The OOB samples gives an estimate of 0.640 for Pearson correlation coefficient and 0.671 for C-index.

2.3 Quantiles for survival time (remission duration) prediction

The remaining question was to choose a survival time (remission duration) for prediction. A typical choice is the median survival time. However, Figure 1 shows that percentiles in interval $[0.1, 0.2]$ seem to be better choices. Again, motivated by model averaging, we chose to average survival quantiles over this interval as the final prediction. The performances, shown by the circled points on the right-most, look better than any single quantile.

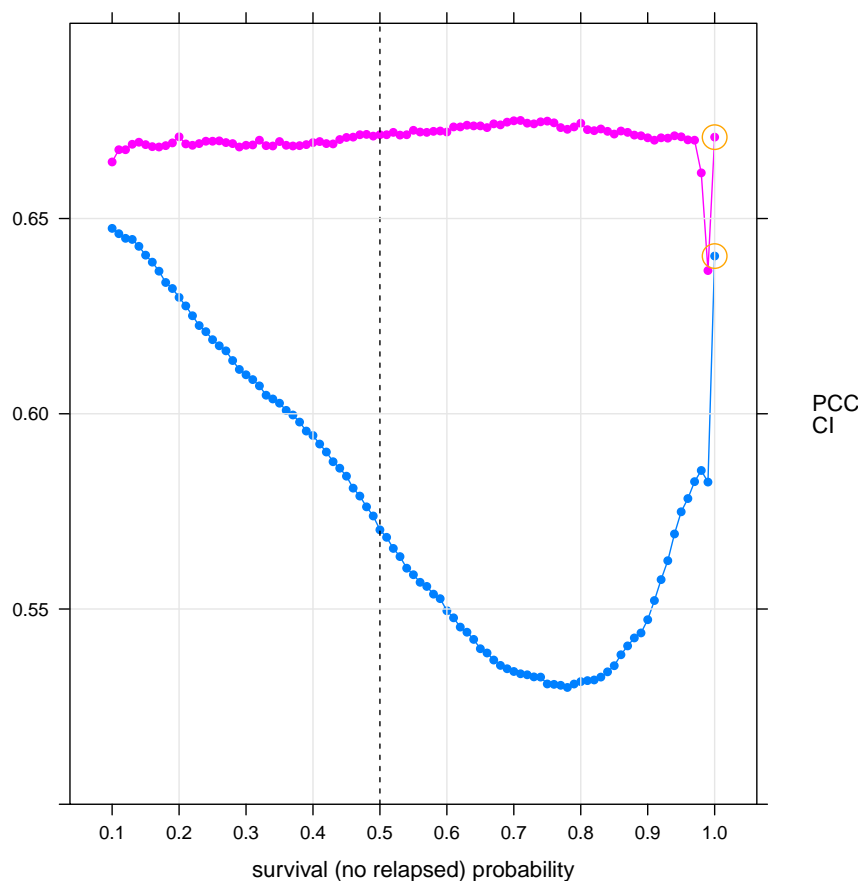


Figure 1: C-index (CI) and Pearson correlation coefficient (PCC) versus chosen survival (no relapsed) probability. The two circled points on the right-most side represent the performance of estimate by averaging over survival probability interval of $[0.1, 0.2]$.

3 Conclusion and Discussion

- The idea of averaging seems to give a better predictive model, though it generally produces a model hard to interpret.
- Our model used five clinical variables, *Age.at.Dx*, *Chemo.Simplest*, *HGB*, *ALBUMIN* and the re-categorized *cyto.cat*. Including additional clinical and/or proteomic variables, de-

terminated by using a minimal-depth, survival random forest model [3], did not substantially improve model performance.

- Interactions and quadratic effects of the five selected variables were added to the model, but no significant improvement was observed.

References

- [1] Grimwade D, Walker H, Oliver F, Wheatley K, Harrison C, Harrison G, Rees J, Hann I, Stevens R, Burnett A, Goldstone A (1998). The importance of diagnostic cytogenetics on outcome in AML: analysis of 1,612 patients entered into the MRC AML 10 trial. The Medical Research Council Adult and Children's Leukaemia Working Parties. *Blood*, 92 (7): 2322-33.
- [2] Bennett JM, Catovsky D, Daniel MT, Flandrin G, Galton DA, Gralnick HR, Sultan C (1976). Proposals for the classification of the acute leukaemias. French-American-British (FAB) co-operative group. *Br J Haematol* 33 (4): 45-8. doi:10.1111/j.1365-2141.1976.tb03563.x
- [3] Ishwaran H., Kogalur U.B., Chen X. and Minn A.J. (2011). Random survival forests for high-dimensional data. *Stat. Anal. Data Mining*, 4, 115-132
- [4] Acute Myeloid Leukemia Outcome Prediction Challenge (syn2455683)

Authors Statement

- **Xihui Lin (Eric)**: Model development, validation and discussion; model and algorithm consultant; manuscript writeup.
- **Gregory M. Chen**: Model development, validation and discussion, and manuscript review.
- **Honglei Xie**: Model development, validation and discussion, and manuscript review.
- **Geoffrey A. M. Hunter**: Scientific oversight and discussion, and manuscript review.
- **Paul C. Boutros**: Scientific oversight, funding support, and manuscript review

Corresponding Author: Xihui Lin, Eric.Lin@oicr.on.ca

Sub-challenge #3, Rank #1 Model

A bagged semi-parametric model for predicting overall survival time in AML sub-challenge 3

Xihui Lin : Eric.Lin@oicr.on.ca
Gregory M. Chen : gregorymchen@gmail.com
Honglei Xie : xhonglei2007@gmail.com
Geoffrey A. M. Hunter : Geoffrey.Hunter@oicr.on.ca
Paul C. Boutros : Paul.Boutros@oicr.on.ca

October 13, 2015

Summary

We implemented a bootstrap aggregated (bagged) Cox-like semi-parametric model with carefully selected predictors as a predictive model for overall survival time for sub-challenges 3.

1 Introduction

Why a bagged semi-parametric model

- The performance of the benchmark model using a standard Cox model with five selected clinical predictors is comparable to the top models on the leaderboard and better than our previous models such as survival random forests, boosted quantile regression, and weighted linear model.
- A native average over all submissions in sub-challenge 2 & 3 performs surprisingly well on the leaderboard, so we reasoned that averaging (via bagging) would be a viable strategy to reduce the variance.

Variable selection

- The benchmark model, with an impressive performance, uses only five selected clinical variables.
- From our work on sub-challenge 1, our model performance decreased whenever we incorporated one or more of the protein data, so we omitted this data from our models for sub-challenge 2 & 3 model.
- Based on these observations we started with the selected five clinical variables, i.e., *Age.at.Dx*, *Chemo.Simplest*, *HGB*, *ALBUMIN* and *cyto.cat*.

Missing values

Since there are only a few missing values of the selected variables in the training and testing sets, we simply replace them by the medians and modes for continuous and discrete variables respectively.

2 Methods

2.1 Preprocessing: re-categorizing ‘cyto.cat’

Cytogenetics (*cyto.cat* in AML dataset) is the single most prognostic factor in AML [1]. The distribution of patients across all cytogenetics categories in the AML data is imbalanced. This will negatively affect the performance of a bootstrapped model because some levels might be missing in a bootstrapped sample. Hence, we resolved to re-categorize the cytogenetics category into fewer, more balanced levels.

category	-5	-5,-7	-5,-7,+8	-7	11q23	21	8
frequency	4	8	3	5	7	2	12
category	IM	Misc	diploid	inv16	inv9	t6;9	t8;21
frequency	3	33	90	11	1	2	10

Table 1: Frequencies of levels of *cyto.cat* in training set.

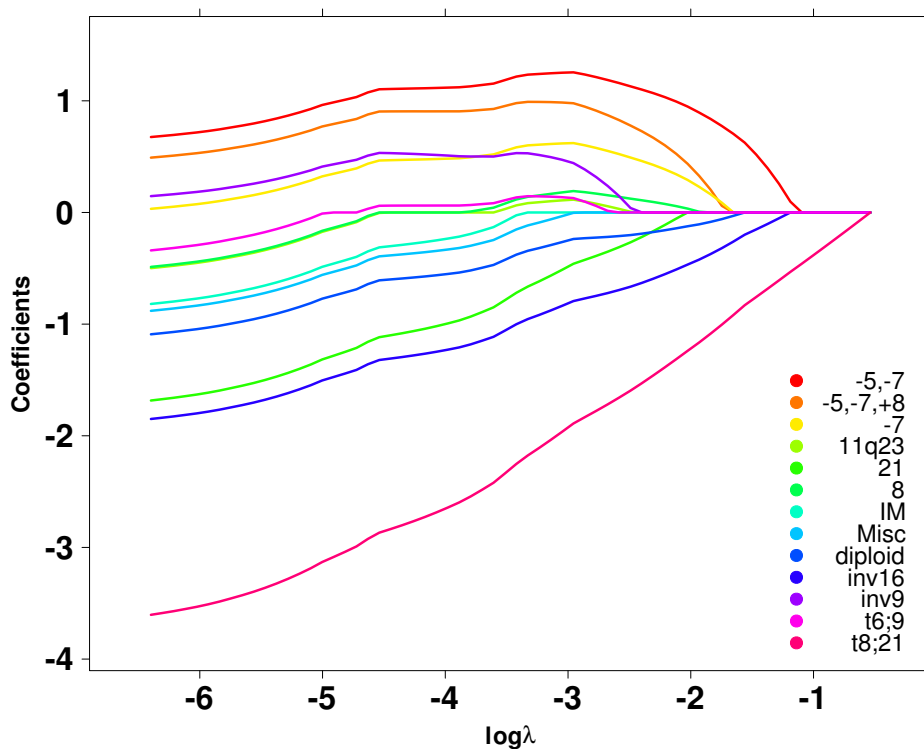


Figure 1: Coefficients vs $\log \lambda$. The numbers inside the figure indicating the index number of levels as in the same order in Table 1, with level ‘-5’ chosen to be the baseline. So ‘-5’ indicates level ‘-5,-7’ and ‘13’ indicates ‘t8;21’. Figure is plotted using BPG [4].

To this end, we fit a Cox model using ‘cyto.cat’ with an elastic-net penalty (R package *glmnet-1.9.8*). We set $\alpha = 0.5$ (the elastic-net penalty) in

$$\lambda(\alpha|\beta| + (1 - \alpha)|\beta|^2/2).$$

Other values of α produced similar shrinkage paths to that in Figure 1. Based on Figure 1, we re-categorized ‘cyto.cat’ into 4 categories in Table 2. The ‘diploid’ category remains the same because it is the most abundant. The ‘t6;9’ category, which is not in the training data, is grouped with ‘t9;22’ for similarity. The ‘inv9’ category is grouped in the baseline category with all other chromosome 9 abnormalities because there is only one sample with this category in the training data. Lastly, the level ‘-7,+8’ in the test sets is thought to be similar to ‘-5,-7,+8’ and is consistent with the cytogenetic categories in Grimwade *et al.* [1] and Bennett [2].

Risk Category	Abnormality	Counts
High	‘-5,-7’, ‘-5,-7,+8’, ‘-7’, ‘-7,+8’	16
Intermediate (baseline)	‘-5’, ‘11q23’, ‘8’, ‘IM’, ‘Misc’, ‘t6;9’, ‘t9;22’, ‘inv9’	62
Intermediate-low	‘diploid’	90
Lower	‘inv16’, ‘t8;21’	21

Table 2: New cytogenetics categories.

2.2 Model

An appropriate model for bagging is one that should be unbiased with high variation. For this purpose, we added some ‘frailty’ terms (inspired by frailty in survival model and the positivity of the selected continuous variables) to the standard Cox proportional hazard model as

$$\lambda(t|x, z) = \lambda_0(t)x^\alpha \exp(x\beta + z\gamma) \quad (1)$$

where x is a vector of positive continuous variates and z is a vector of discrete variables, and

$$x^\alpha := (x_1, \dots, x_k)^{(\alpha_1, \dots, \alpha_k)} := \prod_{i=1}^k x_i^{\alpha_i}.$$

Indeed, equation (1) is equivalent to

$$\lambda(t|x, z) = \lambda_0(t) \exp((\log x)\alpha + x\beta + z\gamma). \quad (2)$$

We draw $B = 500$ bootstrap samples. With each bootstrap sample, model (2) is fitted with R function *coxph* (R-3.1.1, survival-2.37-7). The final prediction from this bagged model is a simple average over all $B = 500$ base models. Out-of-bag (OOB) samples are used to assess the performance, which typically slightly underestimates the performance. The OOB samples gives an estimate of 0.618 for Pearson correlation coefficient and 0.678 for C-index. Similar models with interaction and quadratic terms did not improve model performance.

2.3 Quantiles for survival time prediction

The remaining question was to choose a survival time for prediction. Typically, the median survival time is used, however, percentiles in interval $[0.1, 0.3]$ seem to be better choices (Figure 2). Again, motivated by model averaging, we chose to average survival quantiles over this interval for the final prediction. The performance, shown by the horizontal lines in Figure 2 is better than any single quantile.

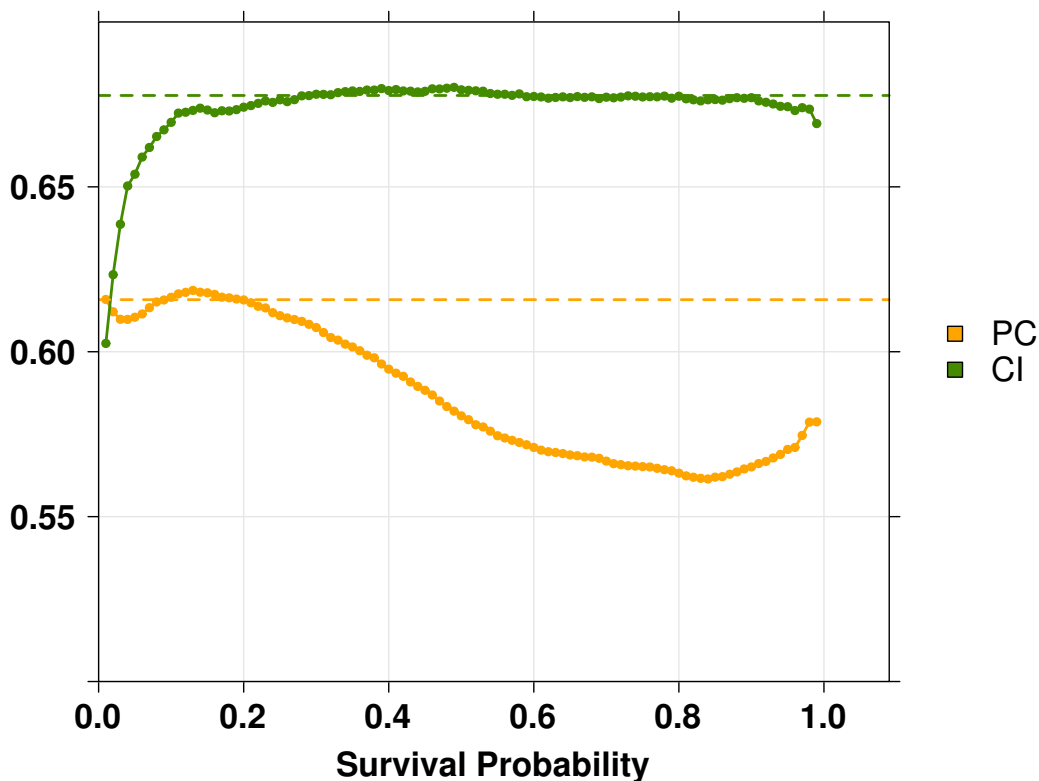


Figure 2: C-index (CI) and Pearson correlation coefficient (PCC) versus chosen survival probability. The horizontal lines represent the performance of estimate by averaging over survival probability interval of [0.1,0.3]. Figure is plotted using BPG [4].

3 Experimental design: which changes improve performance?

Next, we wanted to assess the contribution of each modelling decision (bagging, adding log-transform of continuous variables, and averaging over survival quantiles) to the overall performance of the model. To this end, we performed a 10 fold cross validation with 10 repetitions on all model permutations as outlined in Table 3. The results, shown in Table 4, reveal that all the three model components improved PCC, especially using the mean survival quantiles whereas only bagging significantly improved the CI.

4 Conclusion and Discussion

- Averaging seems to improve model performance at the cost of interpretability.
- Our model used five clinical variables, *Age.at.Dx*, *Chemo.Simplest*, *HGB*, *ALBUMIN* and the re-categorized *cyto.cat*. Including additional clinical and/or proteomic variables, determined by using a minimal-depth, survival random forest model [3], did not substantially improve model performance.
- Interactions and quadratic effects of the five selected variables were added to the model, but no significant improvement was observed.

Bagging	Log Transform	Mean Survival	PCC	CI
0	0	0	0.5988	0.6857
0	0	1	0.6138	0.6868
0	1	0	0.6459	0.6622
0	1	1	0.6534	0.6588
1	0	0	0.6153	0.6969
1	0	1	0.6303	0.7011
1	1	0	0.6538	0.6982
1	1	1	0.6578	0.6990

Table 3: Result of a repeated cross-validation.

		Effect	p-value
PCC	Bagging	0.0113	0.0325
	Log Transform	0.0104	0.0423
	Mean Survival	0.0382	0.0004
CI	Bagging	0.0254	0.0172
	Log Transform	0.0007	0.9221
	Mean Survival	-0.0131	0.1138

Table 4: Result from linear regression on Pearson’s Correlation Coefficient(PCC) and Concordance Index (CI).

- Overall, bagging improves both the PCC and CI, whereas the log-transformed terms and ‘averaging over survival quantile’ only improves the PCC.

References

- [1] Grimwade D, Walker H, Oliver F, Wheatley K, Harrison C, Harrison G, Rees J, Hann I, Stevens R, Burnett A, Goldstone A (1998). The importance of diagnostic cytogenetics on outcome in AML: analysis of 1,612 patients entered into the MRC AML 10 trial. The Medical Research Council Adult and Children’s Leukaemia Working Parties. *Blood*, 92 (7): 2322-33.
- [2] Bennett JM, Catovsky D, Daniel MT, Flandrin G, Galton DA, Gralnick HR, Sultan C (1976). Proposals for the classification of the acute leukaemias. French-American-British (FAB) co-operative group. *Br J Haematol* 33 (4): 45-8. doi:10.1111/j.1365-2141.1976.tb03563.x
- [3] Ishwaran H., Kogalur U.B., Chen X. and Minn A.J. (2011). Random survival forests for high-dimensional data. *Stat. Anal. Data Mining*, 4, 115-132
- [4] P’ng et al. (submitted, 2015), BPG: a package to visualize scientific data. <http://labs.oicr.on.ca/Boutros-lab/software/bpg>
- [5] Acute Myeloid Leukemia Outcome Prediction Challenge (syn2455683)

Authors Statement

- **Xihui Lin (Eric)**: Model development, validation and discussion; model and algorithm consultant; manuscript writeup.
- **Gregory M. Chen**: Model development, validation and discussion, and manuscript review.
- **Honglei Xie**: Model development, validation and discussion, and manuscript review.
- **Geoffrey A. M. Hunter**: Scientific oversight and discussion, and manuscript review.
- **Paul C. Boutros**: Scientific oversight, funding support, and manuscript review

Corresponding Author: Xihui Lin, Eric.Lin@oicr.on.ca

DREAM 9 AML-OPC Consortium

Team 89

Jose M. G. Vilar¹

1 Biophysics Unit (CSIC-UPV/EHU) and Department of Biochemistry and Molecular Biology, University of the Basque Country, Bilbao, Spain

Team Attractor Metagenes

Tai-Hsien Ou Yang¹, Dimitris Anastassiou¹

1 Department of Systems Biology and Department of Electrical Engineering, Columbia University, New York, NY

Team BostonCompBio

Reynald Lescarbeau, Rebecca Lescarbeau

Team Chipmunks.

Honglei Xie¹, Greg Chen¹, Xihui Lin¹, Geoffrey Hunter¹

1 Ontario Institute for Cancer Research, Toronto, ON, Canada

Team Clinical Persona

Ljubomir Buturovic¹, Damjan Krstajic^{1,2}, Alejandrina Pattin¹

1 Clinical Persona Inc, East Palo Alto, CA, USA

2 Research Centre for Cheminformatics, Beograd, Serbia

Team Creighton

Chad J. Creighton^{1,2}

1 Department of Medicine and Dan L. Duncan Cancer Center, Baylor College of Medicine, Houston, TX, USA

2 Department of Bioinformatics and Computational Biology, The University of Texas M. D. Anderson Cancer Center, Houston, TX, USA

Team CS

Sunho Park¹, Minsoo Kim¹, Alan Estrada¹, Jae-Ho Cheong^{2,3}, Tae Hyun Hwang¹

1 Department of Clinical Sciences, University of Texas Southwestern Medical Center, Dallas, TX, USA

2 Department of Surgery, Yonsei University College of Medicine, Seoul, South Korea

3 Department of Biochemistry & Molecular Biology, Yonsei University College of Medicine, Seoul, South Korea

Team EPD

Sunil Kumar^{1,2}, René Dreos², Giovanna Anbrosini^{1,2}, Philipp Bucher^{1,2}

1 The Swiss Institute for Experimental Cancer Research (ISREC), School of Life Sciences, EPFL, Lausanne, Switzerland

2 The Swiss Institute of Bioinformatics (SIB), EPFL, Lausanne, Switzerland

Team EvoMed

Li Liu¹

1 Department of Biomedical Informatics, Arizona State University, Tempe, AZ, USA

Team ICM CUDA Dreamers

Paweł Żuk¹, Antoni Rościszewski¹, Rafał Niemiec², Mariusz Wrzesień², Witold Rudnicki¹

1 Interdisciplinary Centre for Mathematical and Computational Modelling, University of Warsaw, Warsaw, Poland

2 University of Information Technology and Management in Rzeszów, Rzeszów, Poland

Team JamesMcM

James McMurray¹

1 Max Planck Institute for Intelligent Systems, Tübingen, Germany

Team JP

Jinpu Li¹

1 University of Science and Technology of China, Hefei, Anhui, China

Team JTNL

Tom Ronan¹, Jennifer Flynn², Kristen Naegle¹

1 Department of Biomedical Engineering, Washington University in St. Louis, St. Louis, MO, USA

2 Division of Biology and Biomedical Sciences, Washington University in St. Louis, St. Louis, MO, USA

Team Jyothi

Jyothi Korra¹

1 Christ University, Bengaluru, Kanataka, India

Team KAATZ-at-OSU

Kelly Regan¹, Tasneem Motiwala¹, Daniel Morgan¹, Zachary Abrams¹, Andrea Peabody¹, Andrew Fitzgerald¹

1 Department of Biomedical Informatics, The Ohio State University College of Medicine, Columbus, OH, USA

Team nadal

Daniel Kim

Team Naoned e Breizh

Loic Champion^{1,2}

1 Integrated Center of Oncology, Biometrics Unit, St-Herblain, France

2 Cancer Research Center Nantes-Angers, Nantes, France

Team sg_139

Subharup Guha¹, Veerabhadran Baladandayuthapani^{2,3}

1 Department of Statistics, University of Missouri, Columbia, MO, USA

2 Department of Biostatistics, The University of Texas MD Anderson Cancer Center, Houston, TX, USA

3 Department of Biostatistics, Rice University, Houston, TX, USA

Team Snail

Tiziana Sanavia¹, Barbara Di Camillo¹

1 Department of Information Engineering, University of Padova, Padova, Italy

Team ssss

Seyyed A. Fatemi¹, Anthony Kuh¹

1 Electrical Engineering Department, University of Hawaii at Manoa, Honolulu, HI, USA

Team SWlab

Kimberly Batten¹, Jerry Shay¹, Woodring Wright¹

1 UT Southwestern Medical Center at Dallas, Dallas, TX, USA

Team SWP

Scott W. Piraino

Team test_ho

Maryam Hosseini¹, Narayana Santhanam¹

1 Electrical Engineering Department, University of Hawaii at Manoa, Honolulu, HI, USA

Team TT

Hao Tang¹, Xiao Zang¹, Tao Wang¹, Guanghua Xiao¹, Yang Xie¹

1 University of Texas, Southwestern Medical Center, Dallas, TX, USA

Team YL

Yashu Liu¹, Jieping Ye¹, Sen Yang¹, Tao Yang¹

1 Arizona State University, Tempe, AZ, USA

Team yoda

Maciej Fronczuk¹, Weiyi Gu¹, Ling-Hong Hung¹, Vivian G. Oehler², Kiyana Zolfaghar¹, Ka Yee Yeung¹

1 Center for Data Science, Institute of Technology, University of Washington, Tacoma, WA, USA

2 Clinical Research Division, Fred Hutchinson Cancer Research Center, Seattle, WA, USA